REVIEW OF 30 YEARS OF SCARAB RE-ENTRY BREAK-UP ANALYSIS

P. Kärräng, T. Lips, A. Breslau, and B. Fritsche

HTG – Hypersonic Technology Göttingen GmbH, Germany, Email: p.kaerraeng@htg-gmbh.com

ABSTRACT

In recent years, the number of satellites and rocket stages in Earth orbit has significantly increased, most of which will re-enter Earth's atmosphere. As these objects re-enter, they will heat up, ablate, and break up into many fragments, some fragments will survive to ground, posing a risk to people and property.

The risk associated with such a re-entry can be assessed with destructive re-entry simulation tools. ESA's SCARAB (Spacecraft Atmospheric Re-entry and Aerothermal Breakup) is a spacecraft-oriented re-entry break-up simulation code. The development of SCARAB started under the lead of HTG (Hypersonic Technology Göttingen) in 1995. The goal of this development was an approach to cover all the multidisciplinary aspects of a re-entry in one tool, and to become able to simulate the destructive re-entry of a full spacecraft with relatively high level of detail with the computational resources available back then.

SCARAB has been under continuous development for three decades, with numerous applications across a wide range of use cases. SCARAB has been used in re-entry risk assessment, plasma wind-tunnel test rebuilding, design-for-demise on platform- and equipment-level, controlled re-entry including explosion analysis, meteoroid ablation simulation, planetary protection for Mars, and airborne observation campaigns. SCARAB has also been used in many international re-entry comparison campaigns. These endeavors have created a large archive of re-entry simulations from various satellite designs and rocket bodies.

This paper provides an overview of the different ways SCARAB has been used over the last 30 years, along with a summary of the results archive. These results have been used to develop a stochastic re-entry casualty risk model for the number and size of surviving fragments from re-entering spacecraft.

1. INTRODUCTION

The need for destructive re-entry risk analysis in the modern space economy has become undeniable. There are currently more than 10,000 active satellites in orbit [1]. Numerous constellations, each with up to thousands of satellites are being deployed, or are in planning stages [2]. All these satellites have to be disposed of at the end of their operation. Currently, atmospheric re-entry is the most common way of disposal.

An atmospheric re-entry can either be controlled, where the time and place of re-entry is actively ensured, or uncontrolled where the impact location can occur anywhere along the satellite's sub-track at an unknown time. Semi-controlled re-entries are becoming more popular and show great potential in reducing the risk for large constellations to acceptable levels [3]. In this type of re-entry the possible impact location is not exactly determined, but instead limited to within a fraction of an orbit. This allows operators to phase the entry to a ground track where it would pose a minimal risk to people on-ground.

The process of spacecraft breakup during re-entry is complex [4, 5, 6]. This is due to the dynamic environment that the object encounters during the re-entry. At first, as the object starts to re-enter, the heat flux will be low. However, as it descends deeper into denser parts of the atmosphere the heat flux will increase. The heat absorbed will increase the temperature of the structure, weakening it. Eventually, material degradation and aerodynamic forces will lead to fragmentation when the structural integrity is compromised. The fragments will continue on separate trajectories, either fragmenting further, demising completely, or impacting on ground. If fragments impact with high enough kinetic energy they could pose a risk to people and property on-ground, as well as to aircraft in flight [7, 8, 9].

For ESA projects, compliance with casualty risk requirements has to be assessed with the ESA DRAMA (Debris Risk Assessment and Mitigation Analysis) tool [10]. DRAMA's SESAM (Spacecraft Entry Survival Analysis Module) module is an object-oriented re-entry analysis tool, where the re-entering space object is based on a user-defined fragment list of simple shaped objects (e.g. sphere, box, cylinder, etc.). If needed, ESA's more detailed spacecraft-oriented re-entry tool SCARAB can be used for ground risk assessment.

With the increasing number of satellites in orbit, also the frequency of re-entries will increase. Predictions for this challenge from a long-term re-entry risk assessment point

Proc. 9th European Conference on Space Debris, Bonn, Germany, 1–4 April 2025, published by the ESA Space Debris Office
Editors: S. Lemmens, T. Flohrer & F. Schmitz, (http://conference.sdo.esoc.esa.int, April 2025)

of view requires a stochastic re-entry casualty risk model for the number and size of surviving fragments from re-entering spacecraft. One primary goal of this review was to develop such a model based on the history of SCARAB simulations from the last 30 years.

Additionally, some general statements about re-entries have been established in the re-entry safety community over the years, such as the following engineering "*rules-of-thumb*":

- *Spacecraft below* ~ 400 *kg are fully demisable*
- *10–40% of the re-entering mass survives to ground*
- *The main breakup of a spacecraft occurs at* $\sim$*78 km*

Some of these statements are based on little evidence, others rely on old data. Consequently, another goal of this review was to investigate if these common assumptions can be verified based on historical SCARAB result data. And if not, to provide recommendations for updates.

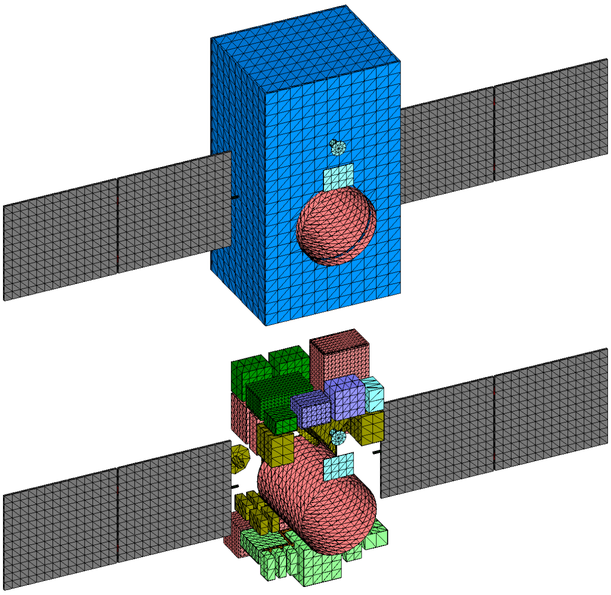

Figure 1. SCARAB model (example)

2. SCARAB OVERVIEW

SCARAB (Spacecraft Atmospheric Re-Entry and Aerothermal Breakup) is a spacecraft-oriented software tool allowing the analysis of mechanical and thermal destruction of spacecraft and other objects during re-entry [11].

Since 1995, SCARAB has been developed under ESA contracts led by HTG (Hypersonic Technology Göttingen) with support from other European and international partners. The software development has evolved over time, based on lessons learned from preceding software versions, upgrades and specific re-entry analyses performed for satellite missions, space stations and launcher programs.

SCARAB is an integrated software package (six degrees-of-freedom flight dynamics, aerodynamics, aerothermodynamics, thermal- and structural analysis) used to perform re-entry risk assessments (quantification, characterization and monitoring of surviving fragments during re-entry). SCARAB constructs a 3D geometric model of the spacecraft (see Fig. 1), with volume panel grid which serves as foundation for the computation of aerodynamic forces and torques experienced by the spacecraft during re-entry, as well as being the basis for the thermal computation.

The software has been validated with in-flight measurements, re-entry observations and wind-tunnel experiments, and it has been compared to other re-entry prediction tools of the international community.

SCARAB has also been used to support experimental demise test campaigns in plasma wind-tunnels by providing numerical test predictions and rebuildings.

3. SCARAB ARCHIVE

SCARAB has now been used for destructive re-entry analyses for three decades. These activities have created a large result archive, which currently includes analyses for 37 satellite and launcher projects with more than 90 unique design iterations and over 1,000 simulations. The amount of data in the SCARAB archive adds up to approximately 3.4 TB compressed, or $\sim$ 34 TB uncompressed.

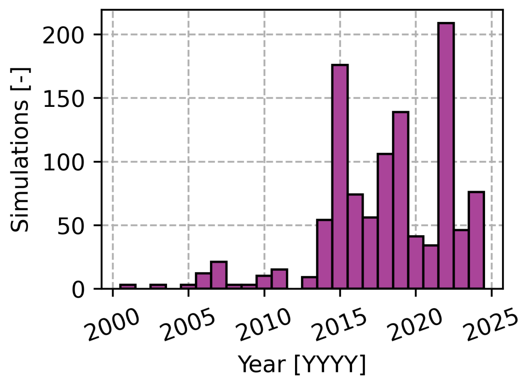

Figure 2. SCARAB simulations performed per year

Fig. 2 shows the number of simulations performed per year which are included in the archive. The earliest simulation in the archive is from 2001, and the majority of simulations have been performed since 2015. SCARAB simulations have also been done in the years 1995–2000, but these are not included in the database as they were performed with SCARAB version 1.0 which is not directly comparable with later versions of the software. The

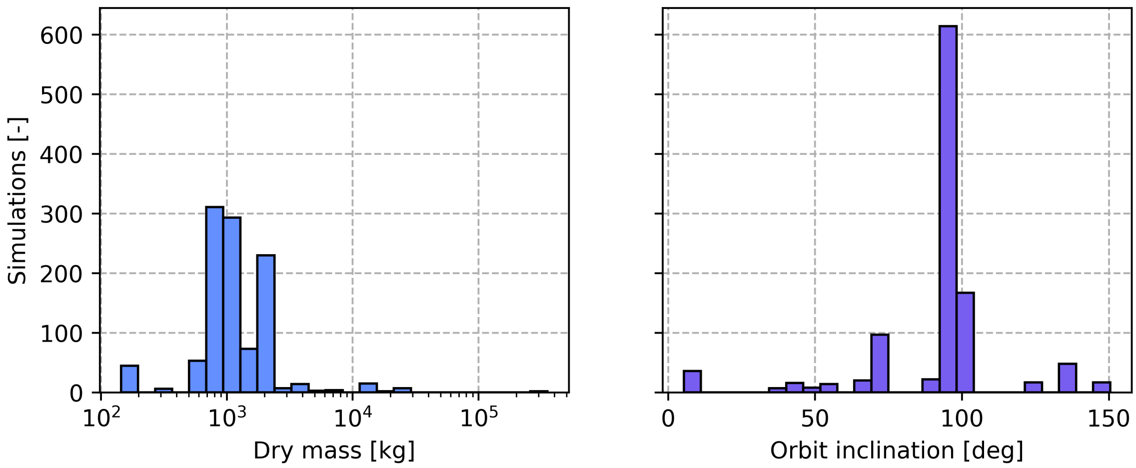

Figure 3. Histogram for dry mass (left) and orbit inclination (right) of re-entry objects in the SCARAB archive

majority of simulations in the archive were performed with SCARAB 3.0/3.1L, while only few were produced with SCARAB 1.5 [11].

A comprehensive examination of the data available in the SCARAB archive has been done. The following sections summarize the results of this data analysis. The findings have been organized into three main categories: in orbit, during re-entry, and on-ground.

3.1. In Orbit

The first aspect to examine for the archived data is the identification of potential biases stemming from some specific ranges covered by the archive, such as re-entry mass, orbit inclination and spacecraft composition.

The left part of Fig. 3 shows a histogram for the number of simulations performed with specific initial dry masses. This figure shows a substantial range of initial dry masses, spanning from around 200 kg up to more than 300 tons. This broad range demonstrates the diversity of re-entering objects available in the database. There are two prominent peaks at around 1,000 kg and 2,000 kg. The largest number of simulations have been performed for objects with approximately 1,000 kg.

The initial inclinations of the re-entry objects in the SCARAB archive are shown on the right side of Fig. 3. Again, the histogram shows a wide range of inclinations, ranging from around 20 deg up to 150 deg. There is a pronounced peak at approximately 98 degrees for re-entries from polar orbits.

The material mass fractions modeled for the spacecraft in the archive can be seen in Fig. 4. The data in the figure is only for satellites (rocket bodies have been removed as they have completely different material compositions). The materials have been organized into common material categories to get a better overview. The

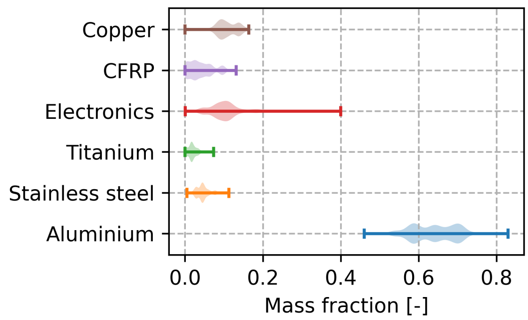

Figure 4. Material composition of satellites in the SCARAB archive

shape of the shaded area indicate the distribution of material fractions for each category, while each distribution is spanning from its minimum to its maximum. The average material fractions are about 64% of Aluminium, 5% of Stainless Steel, 2% of Titanium, 11% of Electronics, 5% of CFRP, and 10% of Copper. This adds up to 97% in total. 3% from this sum are therefore attributed to other materials.

In summary, most simulated spacecraft in the SCARAB archive are satellites in the 1,000–2,000 kg weight class re-entering from polar orbits.

3.2. Re-entry

The archive contains simulations from both controlled and uncontrolled re-entries. However, the majority of the data in the archive is from uncontrolled re-entries.

Fig. 5 shows three plots for the entry trajectories of all the satellites in the archive (rocket stages have again been excluded as they re-enter differently compared to satellites). On the left side, the altitude over time is shown. These

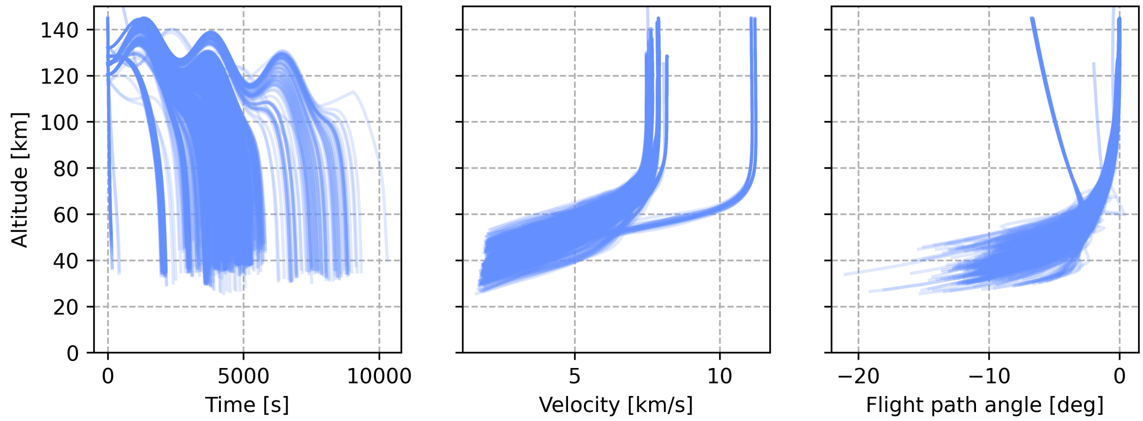

Figure 5. Satellite trajectories in the SCARAB archive

data shows that some objects re-enter the atmosphere in less than one complete orbit, while others require 1–2 orbits before re-entry. The differences in re-entry trajectories can be attributed to different masses and designs. Objects with higher masses, particularly those with smaller projected areas, have ballistic coefficients which allow them to remain in orbit for longer times. However, once a spacecraft is finally captured by the atmosphere it re-enters within a few hundred seconds.

The plot in the middle of Fig. 5 shows altitude over velocity. Two groups can be observed, one with initial velocities around 8 km/s, and another at around 11 km/s. The group re-entering with the lower velocity are typical LEO (Low Earth Orbit) satellites with low eccentricities (i.e. circular orbits). The spread within this group results from different orbit inclinations, which leads to different velocities relative to the co-rotating atmosphere. Re-entering objects with lower inclinations have lower relative velocities, while higher inclinations lead to higher relative velocities. The second group entering at 11 km/s are objects from HEO (High Eccentric Orbits) for which both orbital and relative velocities around the perigee are significantly higher.

The plot on the right of Fig. 5 shows the flight path angle. Most initial flight-path angles are around zero (i.e. horizontally), which is typical for spacecraft on naturally decaying orbits re-entering uncontrolled. There is also another group re-entering steeper (e.g. -6 deg at 120 km). These are again re-entries from HEO in the SCARAB archive.

In summary, most simulated re-entries in the SCARAB archive are for satellites re-entering from LEO after natural decay.

Another aspect of interest during re-entry is the fragmentation process itself. A histogram for the altitude of fragmentation events determined by SCARAB is shown in Fig. 6. Again, this plot includes only the results obtained for satellites as the breakup process of rocket stages is not comparable to the one for satellites. The fragmentation density distribution has two peaks. A smaller peak around 107 km altitude, this is where external equipment and solar panels start breaking off from the satellite. As the satellite descends lower into the atmosphere, the fragmentation density increases until there is a second fragmentation peak at 76–79 km altitude, depending on which statistical metric (mean, median, or mode) is considered.

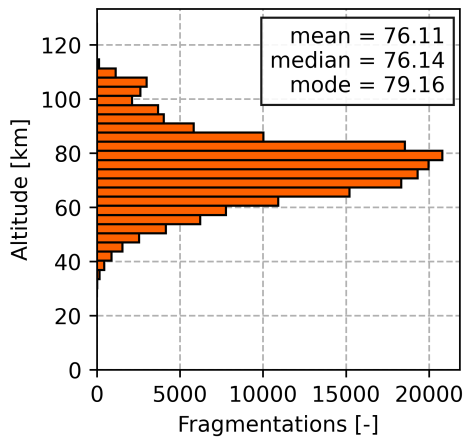

Figure 6. Fragmentation altitude histogram during re-entry for all satellites in the SCARAB archive

3.3. On-Ground

The primary objective of destructive re-entry risk analysis is the identification of fragments which survive to ground. The common metric for quantification of the risk on-ground is the casualty area, which is defined as collision cross-section between surviving fragments and the human body.

The casualty areas extracted from the SCARAB archive for all satellites and rocket stages as function of dry mass can be seen in Fig. 7. Each ellipse in the figure illustrates

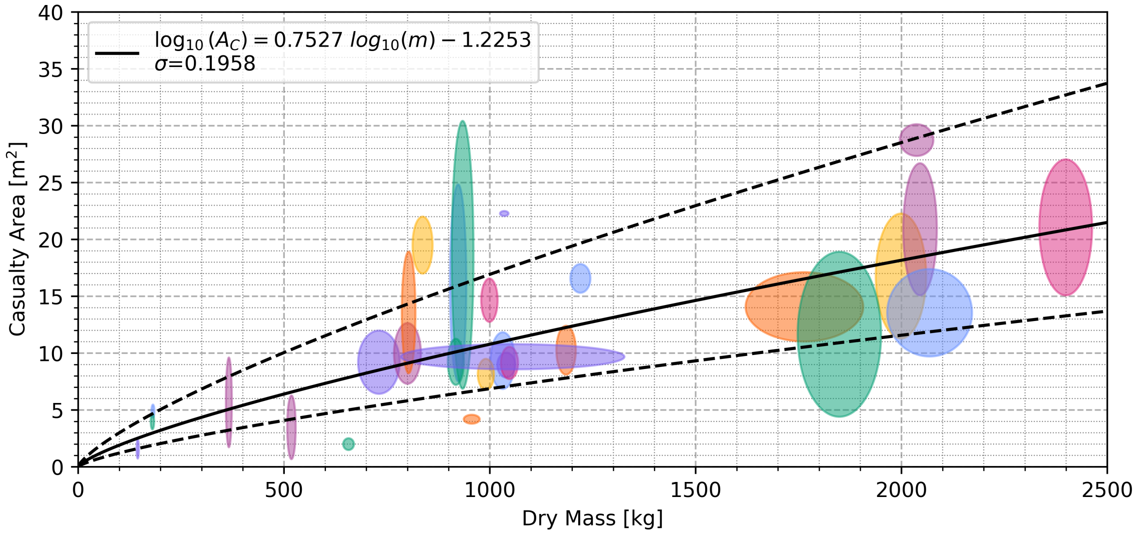

Figure 7. Casualty area as function of re-entry dry mass – SCARAB archive, statistical fit (linear scale)

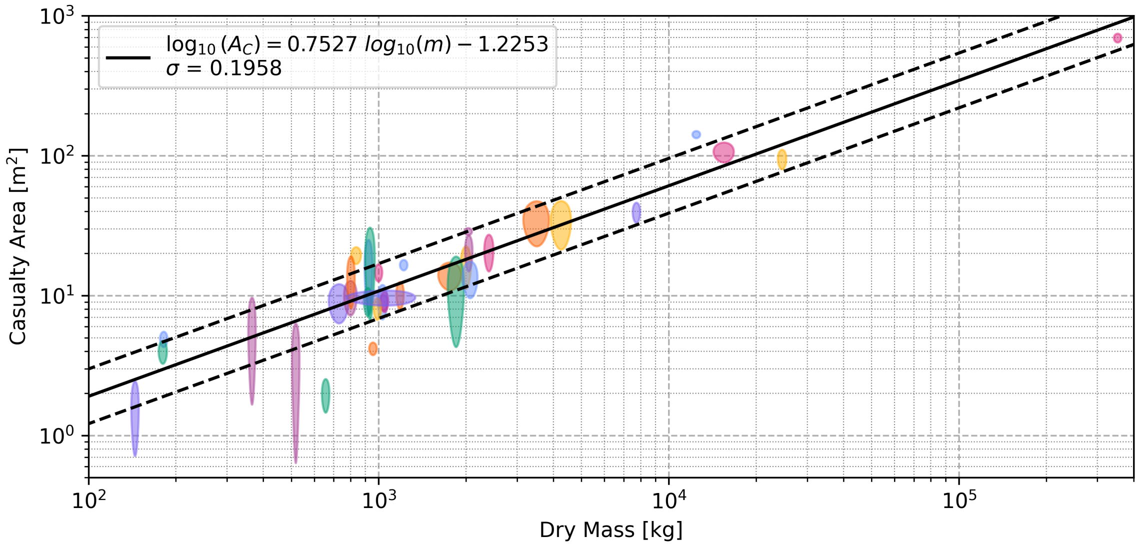

Figure 8. Casualty area as function of re-entry dry mass – SCARAB archive, statistical fit (log-log scale)

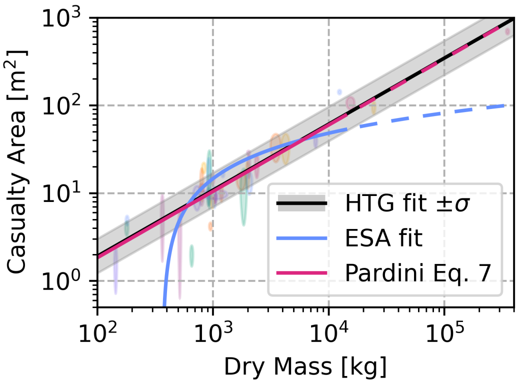

Figure 9. Comparison of statistical fitting functions for casualty area as a function of dry mass (log-log scale)

the results for a specific object (satellite or rocket body) in the archive. The width of the ellipse is one standard deviation of the mass differences between the iterations made for the object (e.g. design changes during the development process or design-for-demise investigations). The height of the ellipse is one standard deviation of the casualty area results for the simulations performed for that object. Visualizing all the objects in the archive on a log-log scale (see Fig. 8) reveals a clear trendline. To find the trendline in the logarithmic-space, linear regression has been performed to get a fit function.

The fit is compared with two previously derived functions in Fig. 9. The functions are shown with solid line for the mass range of the data used to develop the model, the dashed line is extrapolated beyond this range. Generally, the functions are in good alignment for specific mass intervals. The presented fit based on the SCARAB archive (i.e. HTG fit) and the ESA fit [12] are in good alignment within the mass interval between 600 kg and 10,000 kg. And for the one specific fit from Pardini and Anselmo [13], this fit is in very good alignment throughout the entire mass range.

The number of surviving fragments as a function of initial dry mass can be seen in Figs. 10 and 11. The figures show that with increasing mass more fragments are expected to survive. A linear regression in log-log space found a fit for the data, the correlation between number of fragments and initial dry mass is not as good, as for the casualty area fit.

The fraction of surviving mass can be seen in Fig. 12. The figure shows the ratio between the initial and final mass as a function of the initial dry mass. There is no curve fit for this data, however there are three main categories of mass fractions surviving. There is a group of low initial mass spacecraft (<700 kg) where less than 5% of the initial mass survives to ground. Another group of mid-range mass spacecraft (700–2,400 kg) where 10% to 40% of the initial mass survives to ground. And finally above 2,400 kg, 60%–80% of the initial mass survives to ground. The last group is probably skewed to higher surviving mass fractions, due to the fact that these are rocket stages (and a space station), where the re-entries are steeper and the material composition is different from normal satellites.

4. STOCHASTIC RE-ENTRY MODEL

The statistical data analysis presented in the previous section has provided two principal correlations between the re-entry dry mass and the number of surviving fragments n or the on-ground casualty area A_c, respectively:

$$\log_{10}(n) = 0.3761 \cdot \log_{10}(m[\mathrm{kg}]) + 0.0148 \quad (1)$$

$$\log_{10}(A_c[\mathrm{m}^2]) = 0.7527 \cdot \log_{10}(m[\mathrm{kg}]) - 1.2253 \quad (2)$$

Using these equations to determine the *logarithmic mean* number of fragments and casualty area for a given re-entry mass m — $\mu_n(m)$ and $\mu_{A_c}(m)$ — together with the derived standard deviations for these correlations — $\sigma_n = 0.1653$[1] and $\sigma_{A_c} = 0.1958$ — allows to generate random samples by drawing from corresponding log-log normal distributions.

The random samples $(\hat{n}, \hat{A}_c)$ are not independent from each other, but connected via the definition for the casualty area:

$$A_c = \sum_{i=1}^{n} (0.6 + \sqrt{A_i})^2 \quad (3)$$

where A_i are the projected cross-sections of the surviving fragments. Even if there are only infinitesimally small fragments[2] ($A_i \approx 0$ m^2), the minimum casualty area is still $n \cdot 0.36$ m^2. Therefore, random samples for which $\hat{A}_c/\hat{n} < 0.36$ m^2 have to be rejected.

Figs. 14 and 15 are showing example results (orange dots) of this first stochastic casualty area sampling method, both for linear and log-log scale.

However, this direct casualty area sampling method is lacking of further information about the fragments themselves. This can be overcome by using another correlation which has been found by statistical evaluation of the SCARAB archive and further exploitation of results from the previous method:

$$\begin{aligned}\mu_{A_i}(m) = &-0.1180 \cdot \log_{10}(m[\mathrm{kg}])^2 \\ &+ 1.7355 \cdot \log_{10}(m[\mathrm{kg}]) - 5.3468 \end{aligned} \quad (4)$$

$$\sigma_{A_i}(m) = -0.1047 \cdot \log_{10}(m[\mathrm{kg}]) + 0.7094 \quad (5)$$

These two equations provide the mean and the standard deviation of a log-log normal distribution for the projected cross-sections of the surviving fragments. Fig. 13 shows a plot of these two functions. The principle message of this plot is that the average size of the fragments is increasing for higher re-entry masses, while the logarithmic variance around these mean values is decreasing.

[1]This standard deviation has been reduced by 50% from its originally determined value to ensure numerical stability.

[2]This approach does not take into account any kinetic impact energy limits for small fragments.

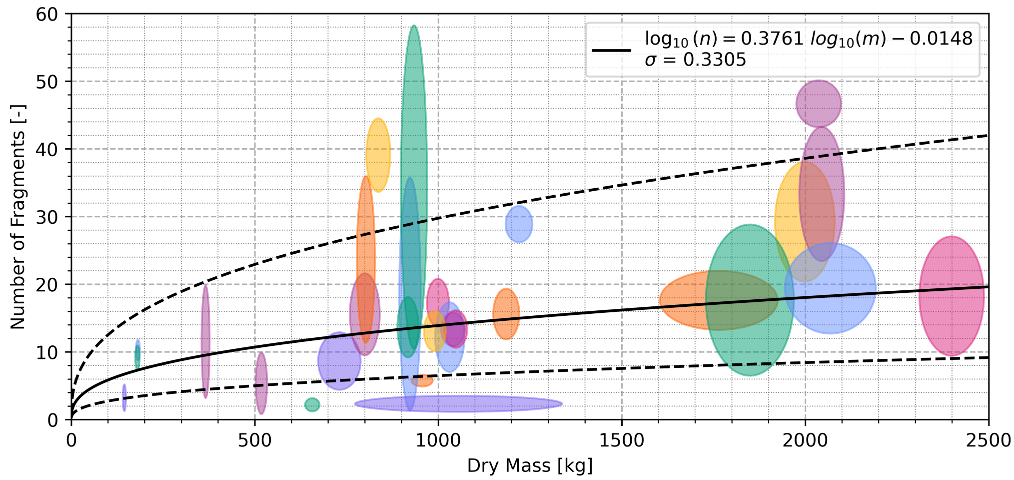

Figure 10. Number of Fragments as function of re-entry dry mass – SCARAB archive, statistical fit (linear scale)

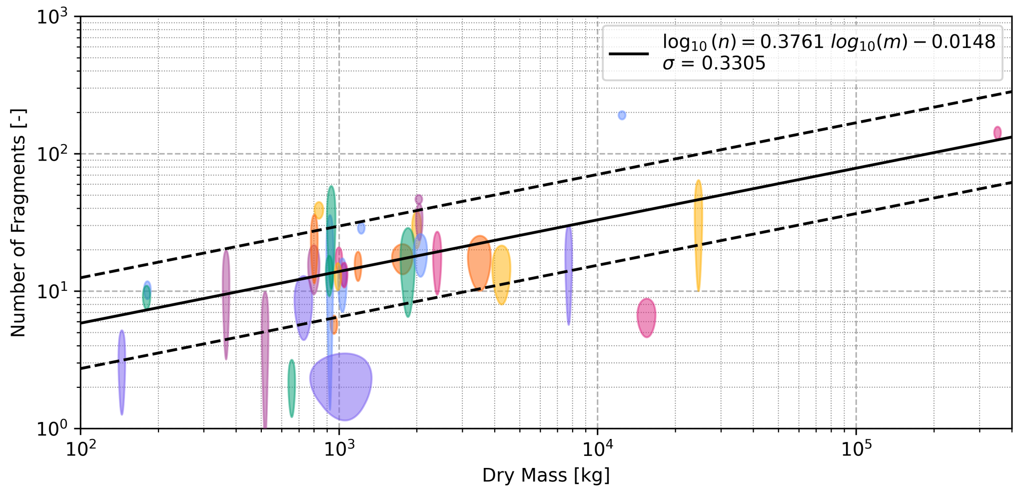

Figure 11. Number of Fragments as function of re-entry dry mass – SCARAB archive, statistical fit (log-log scale)

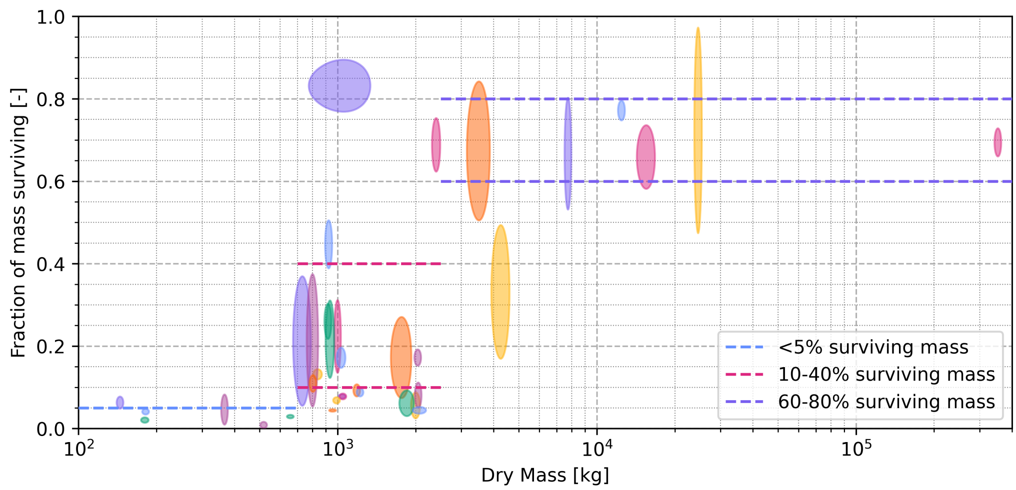

Figure 12. Fraction of initial mass surviving as a function of re-entry dry mass – SCARAB archive

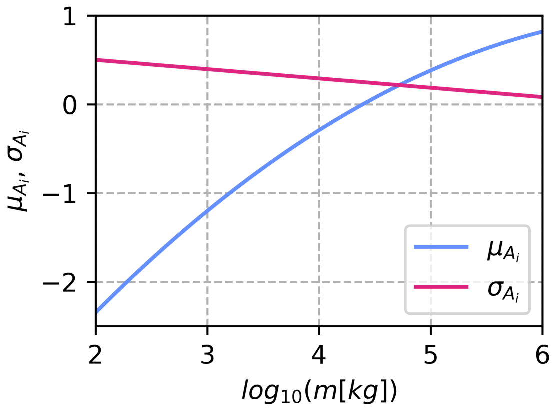

Figure 13. Fragment cross-section distribution

Tab. 1 shows a summary of fragment size ranges for different groups of spacecraft and corresponding mass ranges. The fragment sizes have been computed as the diameters of equivalent spheres for the derived projected cross-sections. This table confirms the plausibility of the model. For normal LEO (Low Earth Orbit) missions, constellations and Earth observation satellites, the fragment size range (including $\pm 1\sigma$ for the projected cross-sections) is in the order of some centimeters up to about half a meter. This corresponds well with SCARAB re-entry simulation results showing, for example, reaction wheel or tank fragments surviving. For the mass class of space stations, meter-sized fragments are predicted by the model which corresponds to big parts of the space station's modules surviving.

Table 1. Fragment size ranges

Group	Mass [kg]	Fragment Size [m]
Micro	[10*;200]	[0.01*;0.20]
Mini	[200;600]	[0.07;0.35]
Small	[600;1,200]	[0.13;0.49]
Medium	[1,200;2,500]	[0.20;0.67]
Intermediate	[2,500;4,200]	[0.30;0.82]
Large	[4,200;5,000]	[0.38;0.88]
Heavy	[5,000;7,000]	[0.42;0.99]
LEO constellations	[200;800]	[0.07;0.40]
LEO EO†	[800;2,500]	[0.16;0.67]
Space stations	[100,000;400,000]	[1.41;2.82]

*Out of validity range (< 100 kg)
†Earth Observation

This approach allows now random sampling of $\hat{n}$ projected cross-sections from which a sample for the casualty area $\hat{A}_c$ can be calculated via Eq. 3. Example results from this second stochastic casualty area sampling method are also shown in Figs. 14 and 15 (green dots), both for linear and log-log scale.

Both stochastic sampling methods provide equivalent results. The second approach is more flexible, for example if one would want to apply other formulas for the calculation of the casualty area, e.g. for collisions with aircraft.

5. SUMMARY AND OUTLOOK

This paper provides an overview of how SCARAB has been used over the last three decades. Historical SCARAB result data have been processed with statistical methods to extract general findings, commonalities and differences, from more than 1,000 re-entry simulations for 37 different spacecraft and rocket stages.

It has been found that two general statements about re-entries – engineering "*rules-of-thumb*" – listed in the introduction should be revised, while the third one was actually confirmed:

- *Spacecraft below* ~ 400 *kg are fully demisable*
  This statement could not be confirmed. Full demisability in general can (most likely) only be assumed for CubeSats with less than 6U ($m < 12$ kg).
- *10–40% of the re-entering mass survives to ground*
  This statement is correct for the gross average of all processed simulations (26%). Data analysis also confirmed that the range of 10–40% is quite valid for satellites in the 700–2,400 kg mass class. Below 700 kg, surviving mass fractions of ∼5% have been extracted. Above 2,400 kg, 60–80% of the re-entry mass can be expected to survive. The latter is most likely driven by the different re-entry breakup and demise behavior of rocket stages compared to satellites.
- *The main breakup of a spacecraft occurs at ∼78 km*
  This statement is correct. Depending on the statistical metric considered, a range of 76–79 km has been derived for the "main" breakup altitude. This is the altitude where the fragmentation frequency is most intense in SCARAB simulations.

Clear analytical correlations between the re-entering mass and the corresponding number of fragments on ground as well as the casualty area have been found. These correlations have been compared with others in the literature. Two stochastic models have been proposed for application in long-term risk assessment.

The SCARAB archive will continue to grow in the coming years. Our plan is to regularly update the data processing including new results and to further refine the implemented statistical methods. This is expected to increase confidence in the findings and derived models.

Finally, it should be noted that the results and models presented in this paper are based only on simulations with SCARAB. A comparison of similar data analyses based on results obtained from other re-entry simulation software would be of interest.

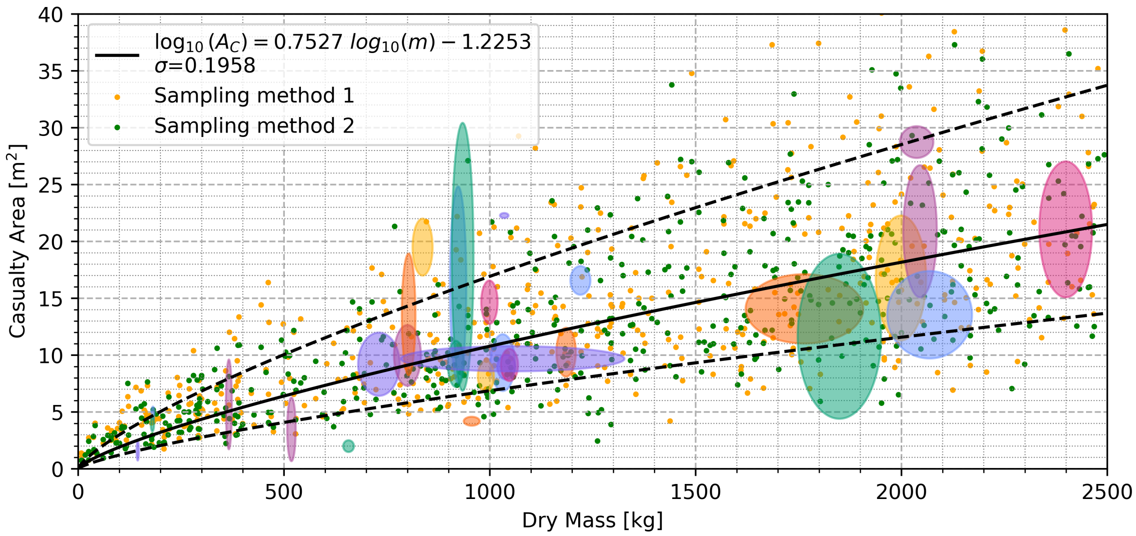

Figure 14. Casualty area as function of re-entry dry mass – SCARAB archive, statistical fit, and stochastic sampling (linear scale)

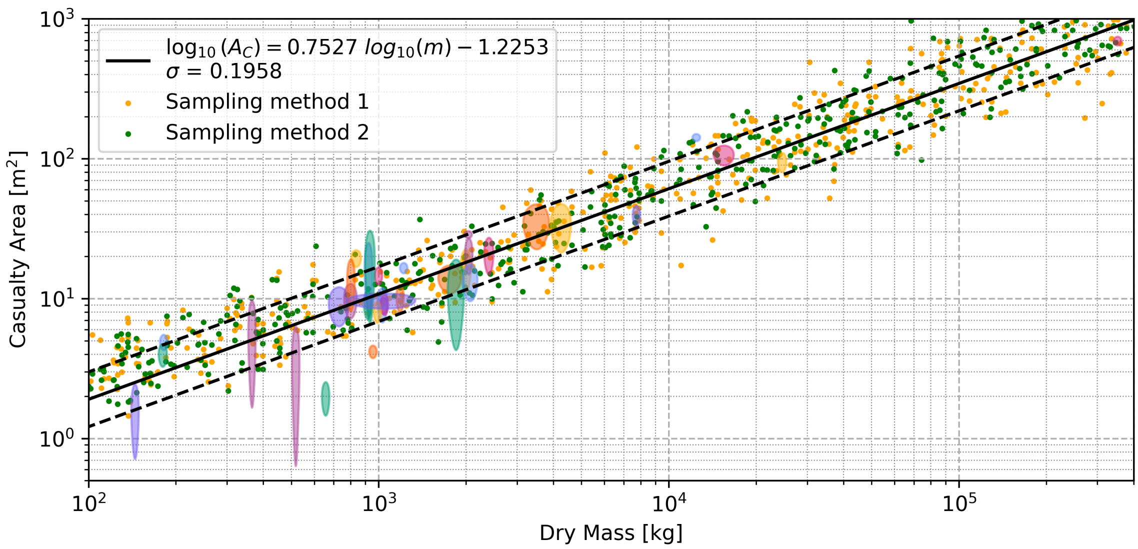

Figure 15. Casualty area as function of re-entry dry mass – SCARAB archive, statistical fit, and stochastic sampling (log-log scale)

ACKNOWLEDGEMENTS

The authors wish to thank all members of the ESA Space Debris Office, Clean Space Initiative and Space Safety Program for their support in the various projects developing and using SCARAB over the years, as well as all our customers and partners from industry and academia.

REFERENCES

1. ESA Space Debris Office (2024). *ESA's Annual Space Environment Report*, GEN-DB-LOG-00288-OPS-SD, Issue 8.0
2. Ailor, W. (2022). Protecting the LEO environment. *Journal of Space Safety Engineering*, 9(3), 449-454
3. Lips T. et al. (2017). Casualty Risk Reduction by Semi-Controlled Re-entry, *Proceedings of the 9th IAASS Conference*, Toulouse, France
4. Fritsche B. et al. (1997). Spacecraft Disintegration During Uncontrolled Atmospheric Re-Entry, *Proceedings of the Second European Conference on Space Debris*, ESA SP-393, Darmstadt, Germany
5. Fritsche B. et al. (2001). Computation of destructive satellite re-entries, *Proceedings of the Third European Conference on Space Debris*, ESA SP-473, Darmstadt, Germany
6. Klinkrad, H. (2006). Space Debris: Models and Risk Analysis, *Springer Science Business Media*
7. Omaly, P. et al. (2025). Hazards associated with reentry, *Acta Astronautica*, 228, 246-252
8. Pardini, C. and Anselmo, L. (2024). The risk of casualties from the uncontrolled re-entry of spacecraft and orbital stages, *Journal of Space Safety Engineering*, 11(2), 181-191
9. Hook, C. at al. (2024). Uncontrolled reentries of space objects and aviation safety, *Acta Astronautica*, 222, 69-80
10. ESA (2017). ESA Re-entry Safety Requirements, ESSB-ST-U-004, Issue 1.0
11. Lips T. et al., (2007). Re-entry Risk Assessment for Launchers - Development of the New SCARAB 3.1L, *Proceedings of the Second IAASS Conference*, ESA SP-645, ESA Communication Production Office, Noordwijk, The Netherlands
12. ESA (2023). ESA Space Debris Mitigation Compliance Verification Guidelines, ESSB-HB-U-002, Issue 2.0
13. Pardini, C. and Anselmo, L. (2022). The kinetic casualty risk of uncontrolled re-entries before and after the transition to small satellites and mega-constellations, *Journal of Space Safety Engineering*, 9(3), 414-426